

Small-scale oxygen fluxes and remineralization in sinking aggregates

Helle Ploug¹

Marine Biological Laboratory, University of Copenhagen, Strandpromenaden 5, DK-3000 Helsingør, Denmark

Abstract

Sinking aggregates are the major component of the vertical particulate flux in most regions of the ocean. Controlling factors for aggregate remineralization rates and solute exchange with the surrounding water, however, are poorly quantified because of few empirical data. To study the role of flow and diffusion on aggregate remineralization rates, oxygen distributions were mapped within and around aggregates by use of microelectrodes in a flow field similar to that experienced by sinking aggregates. The oxygen distribution was asymmetrical with a wake of undersaturated water at the rear (downstream) of the aggregates. Oxygen concentrations within the aggregates were >80% of air saturation. The diffusive fluxes of oxygen at the aggregate-water interface were similar along the equator and at the downstream pole for a wide range of different aggregate sources (field-sampled diatom aggregates, lab-made diatom aggregates, aggregates formed from freeze-thawed diatoms, and zooplankton detritus aggregates) measured at various temperatures. Remineralization rates were reaction limited and, hence, determined by substrate quality and quantity rather than by transport-limited oxygen supply during sedimentation at ambient oxygen concentrations above $\sim 25 \mu\text{M}$.

Aggregates of phytoplankton and detritus colonized by microorganisms are common features in the pelagic environment of lakes, rivers, and the ocean (Alldredge and Silver 1988; Eisma 1993; Grossart and Simon 1993). Bacteria, flagellates, and ciliates are up to 10,000-fold more concentrated on aggregates compared to a similar volume of ambient water (Caron et al. 1986). Aggregate sinking velocities range between 20 and 200 m d^{-1} (Alldredge and Gotschalk 1988), and sinking aggregates comprise a significant component of the flux of organic matter formed in the euphotic zone and exported to sediments in most regions of the ocean, i.e., the draw down of atmospheric CO_2 into the deep ocean and sediments (Shanks and Trent 1980; Fowler and Knauer 1986). However, the vertical flux of organic matter below the euphotic zone decreases significantly with increasing water depth, and the organic matter that reaches the sediment is partly solubilized and remineralized through microbial degradation during the sedimentation process (Lee and Wakeham 1988).

Solubilization and remineralization processes of the organic substrates often imply that the concentrations of oxygen, silicic acid, and dissolved organic carbon (DOC) within aggregates are significantly different from those in the bulk water (Alldredge and Cohen 1987; Brzezinski et al. 1997; Alldredge 2000), and the measured influx of oxygen and efflux of dissolved combined amino acids between the aggregates and the surrounding water suggest an efficient mass transfer at the aggregate-water interface (Smith et al. 1992;

Ploug et al. 1997; Ploug and Jørgensen 1999). However, controlling factors for small-scale fluxes of solutes between the aggregate and surrounding water and aggregate remineralization rates during sedimentation are poorly quantified because of insufficient experimental techniques. Alternatively, mass transfer theory has been applied to estimate interface fluxes and/or diffusion rates within aggregates on the assumption that fluxes of solutes to and from aggregates are transport limited (Csanady 1986; Brzezinski et al. 1997).

The recent development of a vertical flow system in which aggregates can be stabilized in the suspended phase by an upward directed flow velocity that opposes and balances the sinking velocity of individual aggregates has now enabled direct quantification of flow and diffusion around these during sinking (Ploug and Jørgensen 1999). The measured gradients of flow and solutes in the vicinity of aggregates in this flow system have been shown to agree with those predicted by mass transfer theory, independent of transport limitation of the biological processes (Kiørboe et al. 2001).

In the present study, small-scale oxygen dynamics and interface fluxes were analyzed in aggregates of different sources, sizes, and sinking velocities at various temperatures. The measured oxygen fluxes were compared with those predicted by mass transfer theory at transport or reaction limitation of remineralization rates in sinking aggregates, in order to examine whether remineralization rates are indeed diffusion limited during sedimentation.

Materials and methods

Theoretical considerations—The relative importance of inertial and viscous forces acting in the vicinity of a sinking particle is expressed by the Reynolds number:

$$\text{Re} = \frac{Ur_o}{\nu} \quad (1)$$

where U is the sinking velocity, r_o the particle or aggregate radius, and ν the kinematic viscosity of seawater. The viscous forces dominate the water movement if Re is < 0.1 and

¹ Present address: Max Planck Institute for Marine Microbiology, Celsiusstr. 1, D-28359 Bremen, Germany (hploug@mpi-bremen.de).

Acknowledgements

This study was supported by a grant from the Carlsberg Foundation (J. 980511/20-513 and 990513/20-542) and the Danish Natural Science Research Council (J.9801391). I am grateful to Hans-Peter Grossart, who collected diatom aggregates by SCUBA and commented on an earlier version of the manuscript. Zooplankton detritus was kindly provided by Thomas Kiørboe, who also commented on an earlier version of the manuscript.

the streamlines are symmetrical upstream and downstream of a sinking particle (i.e. Stokes "creeping" flow). The streamlines become increasingly asymmetrical and the flow laminar at higher Re, where the inertial forces dominate over viscous forces (Kiørboe et al. 2001). The Reynolds number for most sinking aggregates >0.5 mm ranges from 0.1 to 20 (Alldredge and Gotschalk 1988).

The relative increase in mass transfer due to flow in the vicinity of sinking aggregates compared with that to suspended, nonsinking aggregates in stagnant water is described by the (bulk) Sherwood number (Sh), and it increases with increasing Re (Kiørboe et al. 2001):

$$\text{Sh} = 1 + 0.619\text{Re}^{0.412}\text{Sc}^{1/3} \quad (2)$$

where Re is defined with respect to aggregate radius, Sc is the Schmidt number equal to ν/D_w , and D_w is the diffusion coefficient of the chemical solute in the surrounding water. Eq. 2 is valid for all $\text{Re} < 20$, because it is deduced from solving the diffusion/advection equations as well as Navier-Stokes equations numerically for creeping flow and for laminar flow. Turbulent flow occurs at $\text{Re} \gg 20$.

The radial, local diffusive flux of a chemical solute at solid-water interfaces is expressed by (Sherwood et al. 1975)

$$J = -D_w \frac{dC}{dr} = D_w \frac{(C_\infty - C_o)}{\delta_{\text{eff}}} \quad (3)$$

where J is the flux per surface area and dC/dr is the radial concentration gradient at the aggregate-water interface, which can be extrapolated from the concentration at the surface (C_o) to the bulk concentration (C_∞) in order to determine an effective diffusive boundary layer (DBL) thickness, δ_{eff} .

The Sherwood number increases when the average DBL thickness decreases because of flow. The local Sh and DBL thickness vary several-fold from the upstream to the downstream region of a sinking sphere, whereas the local Sh along equator equals that of the bulk Sh—i.e., the local Sh and DBL thickness along equator represent the average values of the surface integrated Sh and DBL thickness around sinking spheres impermeable to flow (Kiørboe et al. 2001). The local flux is dependent on the local DBL thickness during transport limitation of the biological processes. During reaction limitation (i.e., zero order kinetics), however, the flux is constant over the entire aggregate surface, and variations in local Sh therefore reflect variations in surface concentration depending on local DBL thickness. The ratio of local fluxes along the equator and downstream can, thus, be used to determine whether biological processes are transport or reaction limited (Kiørboe et al. 2001).

When the flux is reaction limited and, hence, constant over the entire aggregate surface, the total (area-integrated) flux is described by

$$Q = 4\pi r_0^2 D_w \frac{(C_\infty - C_o)}{\delta_{\text{eff}}} = \text{Sh} 4\pi r_0 D_w (C_\infty - C_o) \quad (4)$$

where Sh is the local Sherwood number, which can be expressed as the ratio of the aggregate radius to the local DBL thickness, and C_o is the local concentration of the chemical solute at the surface of the aggregate.

At transport limitation, the concentration of the chemical

solute is constant over the entire aggregate surface independent on sinking velocity, and the interface flux of the solute increases proportional to the bulk Sh. The total flux is then described by Eq. 4, where C_o is the concentration at the surface and Sh is the bulk Sherwood number described by Eq. 2.

Experiments

Aggregates—Aggregates of different sources were studied. Diatom aggregates were either collected by SCUBA during the spring bloom in Øresund (Denmark) or formed from cultures (*Chaetoceros debilis*, *Skeletonema costatum*) grown at 15°C in a (16:8 h) light:dark cycle on B-medium diluted 10-fold (Hansen 1989) with silicate added to a final concentration of 150 μM . The diatoms from cultures were harvested during the stationary growth phase. The *S. costatum* culture was frozen at -20°C . Immediately after thawing, the culture was diluted 2.5-fold in aged seawater from the deep part of Øresund (salinity: 34‰). The *C. debilis* culture was diluted 2.5-fold with Øresund water, similar to *S. costatum*. Zooplankton detritus, including fecal pellets, were collected from a zooplankton culture (*Acartia tonsa*) grown on *Rhodomonas baltica*. The detritus was diluted and suspended in artificial sea water. Aggregates composed of diatom cultures or zooplankton detritus were formed in separate 0.5-liter tanks on a roller table (Shanks and Edmondson 1989). The speed of the roller table was set at the lowest speed where aggregates were kept in suspension (1.5–2.4 rpm).

Oxygen measurements—Single aggregates were isolated by use of a wide-bore pipette and gently transferred to the chamber of a vertical flow system as described by Ploug and Jørgensen (1999). The flow chamber consists of a 10-cm long, circular plexiglass tube (diameter 5 cm) with a net distended in the middle of the tube. The net provides a relatively uniform flow field across the upper chamber. Aggregates were placed on the net, and the upward directed flow velocity was adjusted by a needle valve until the aggregate was suspended and its sinking velocity was balanced by the flow velocity. Aggregates were either freely suspended above the net or fixed on a thin glass thread above the net during measurements. The fluid motion and solute distribution in the vicinity of the aggregates under this experimental condition are equivalent to those in the vicinity of an aggregate sinking through the water column at a velocity equal to the water flow (Kiørboe et al. 2001). The flow velocities were calculated from the volume of water passing through the chamber per unit time divided by the cross-sectional area of the chamber.

Oxygen concentrations were measured at steady-state by a Clark-type oxygen microelectrode (Revsbech 1989) with a 4- μm -wide sensing tip, a 90% response time of 0.8 s, and a stirring sensitivity of <0.3%. The electrode was attached to a micromanipulator, and its signal was measured by a picoamperemeter connected to a strip chart recorder. It was calibrated in air-saturated and anoxic water with sodium dithionite. Dimensions of individual aggregates and the relative distance between the microelectrode tip and the aggregate

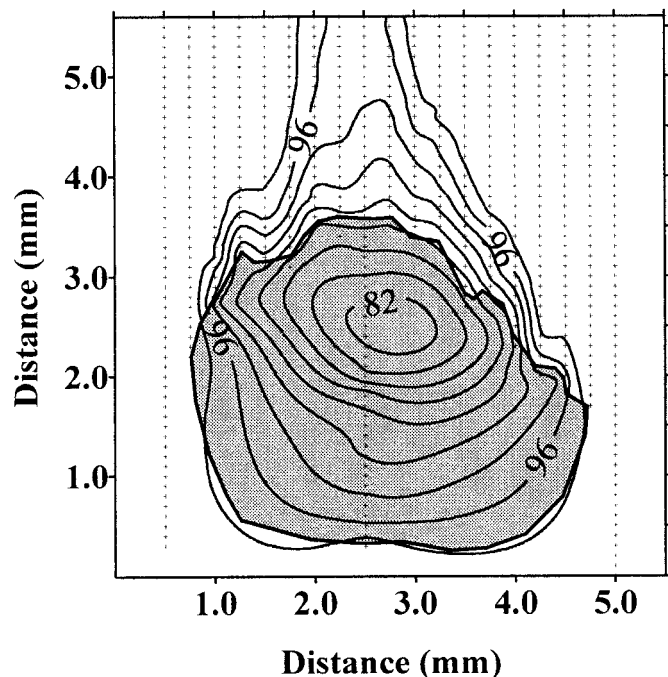


Fig. 1. Isopleths of oxygen distribution (in percentage of air saturation) within and around a ~ 3.5 -mm-large aggregate in an upward-directed uniform flow field with a velocity of 64 m d^{-1} . The crosses represent the measuring points, and the periphery of shaded area is the boundary of the aggregate mapped by the oxygen sensor under the dissection microscope.

gate surface were measured through a dissection microscope with a calibrated ocular micrometer. The water in the flow system was the same as the water in which aggregates had formed, and it was kept at air saturation. The temperature was 7°C , 15°C , or 23°C for field-sampled diatom aggregates, diatom cultures, and zooplankton detritus, respectively. The salinity was 15‰–34‰. At these temperatures and salinity, D for oxygen varies between 1.38×10^{-5} and $2.12 \times 10^{-5} \text{ cm}^2 \text{ s}^{-1}$ and ν varies between 1.47×10^{-2} and 0.99×10^{-2}

$\text{cm}^2 \text{ s}^{-1}$ (Broecker and Peng 1974). For accurate determination of fluxes and DBL thickness, the analytical solutions for oxygen distribution in the DBL were fitted to measured values by applying the solver routine of the spread sheet program Excel 7.0 (Microsoft), as previously described (Ploug et al. 1997).

Results

An example of oxygen distribution mapped from 624 measurements around and within a 3.5-mm large aggregate at a sinking velocity of 64 m d^{-1} is shown in Fig. 1. This sinking velocity is equal to the average sinking velocity of similar-sized aggregates measured in situ (Alldredge and Gotschalk 1988). Oxygen concentrations $\geq 80\%$ of air saturation occurred inside the aggregate because of oxygen respiration by the microbial community living at the surface and within the aggregate. The oxygen minimum zone develops where the diffusion distance to the surrounding water is largest, and it was slightly shifted to the rear of the aggregate because of flow. A wake with oxygen concentrations lower than that of the bulk water occurred at the rear (downstream) of the aggregate, whereas oxygen concentrations along the surface were $\sim 98\%$ of air saturation in the upstream region of the aggregate.

The vertical oxygen distribution through the center of the aggregate and that along the equatorial axis relative to the flow direction are shown in Fig. 2. The radial, diffusive flux of oxygen is proportional to the oxygen gradient at the aggregate-water interface (Eq. 3). The effective DBL thickness was determined by extrapolation of the oxygen gradient at the interface to the bulk water concentration, and it was 1.2 and 0.2 mm downstream and along equator, respectively. The oxygen concentration showed a 12% decrease across 1.2 mm distance downstream (Fig. 2a) and a 2% decrease across 0.2 mm distance along equator (Fig. 2b). The interface diffusive fluxes of oxygen downstream and along equator were similar ($0.17 \text{ nmol O}_2 \text{ mm}^{-2} \text{ h}^{-1}$), because the local concentration difference between that at the surface and the bulk

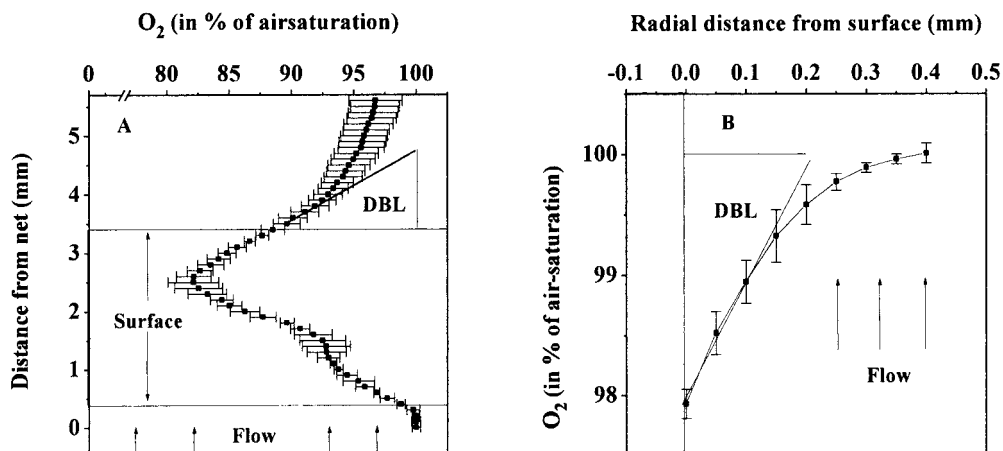


Fig. 2. (A) The vertical distribution of oxygen through the center of the aggregate and (B) the radial distribution along equator of the aggregate. Each measuring point represents the mean value with the standard deviation of the mean value shown as bars ($n = 3$).

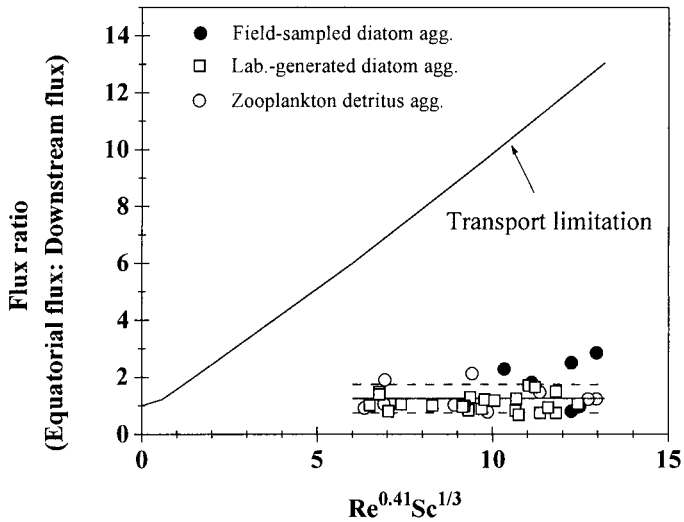


Fig. 3. Measured ratio of the equatorial diffusive flux to that at the downstream pole. The ratio at transport limitation is represented by the solid line. The horizontal lines represent average measured values with the standard deviation of the mean value.

was proportional to the local DBL thickness (Eq. 3). Remineralization rates were, thus, reaction limited rather than transport limited.

The average flux of oxygen at multiple positions in the equatorial plane relative to that at the downstream pole was 1.25 ± 0.50 in aggregates of different sources and at different temperatures (Fig. 3). The ratio of the equatorial fluxes to the downstream flux was up to 12-fold lower than those predicted at transport limitation. This flux ratio is a linear function of $Re^{0.41}Sc^{1/3}$ at transport limitation and intermediate Re (Kiørboe et al. 2001)—hence, it is a nonlinear function of sinking velocity (Eq. 1). It depends on aggregate size, sinking velocity, the temperature-dependent kinematic viscosity of sea water, and the diffusion coefficient of the chemical solute. The aggregate size ranged between 2 and 8 mm, and the sinking velocity ranged between 54 and 200 $m d^{-1}$. The flux ratio and its variation were independent of $Re^{0.41}Sc^{1/3}$ as predicted by reaction limitation of the biological processes. The relatively small variation of flux ratios measured was presumably explained by heterogeneous distribution of microorganisms.

The ratio of aggregate radius to its DBL thickness measured at equator is shown in Fig. 4. The average values increased proportional to the theoretical Sherwood number with increasing aggregate size and sinking velocity (Eq. 2). However, a large scatter was observed at high sinking velocities for aggregates with relatively rough surfaces and where the DBL thickness was in the order of 100–200 μm . The ratio of the aggregate radius to its equatorial DBL thickness increases similar to the bulk Sherwood number at increasing sinking velocities but without an increase of total mass transfer when the biological processes are reaction limited (Kiørboe et al. 2001). Instead, the concentration of solutes, which are consumed within the aggregate, increases at the aggregate surface with increasing sinking velocity.

Oxygen gradients were measured at the aggregate-water

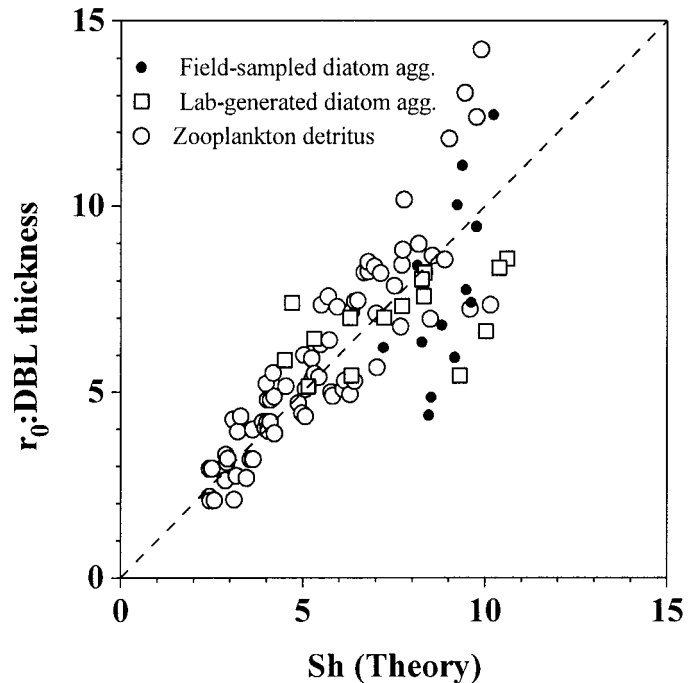


Fig. 4. Measured ratio of r_0 :DBL thickness of equator of different aggregates as a function of the theoretical Sherwood number (Eq. 2). The dotted line represents the 1:1 ratio.

interface along the equator at different sinking velocities, to examine the oxygen dynamics as a function of sinking velocity. Oxygen gradients and fluxes at the aggregate-water interface of three different aggregates composed of zooplankton detritus are shown as a function of sinking velocity in Fig. 5. Oxygen gradients were observed in the surrounding water up to 0.8 mm distance from the aggregate surface at low sinking velocities. At increased sinking velocities, however, the bulk concentration occurred closer to the surface concurrent with an increase in oxygen concentration at the surface (Fig. 5, left panel). The radial flux of oxygen at the aggregate-water interface was, thus, independent of flow and DBL thickness at sinking velocities $>10 m d^{-1}$ (Fig. 5, right panel). The DBL thickness decreased nonlinearly with increasing sinking velocity. It decreased from 400 μm at low sinking velocities to values $\leq 250 \mu m$ independent of aggregate size at sinking velocities $>50 m d^{-1}$. The measured concentration difference between that at the aggregate surface and the bulk (ΔC) normalized to size and flux is shown as a function of the ratio between r_0 and the DBL thickness (Fig. 6). ΔC decreased inversely proportional to the r_0 :DBL thickness ratio as predicted by Eq. 4 when the biological processes are reaction limited and Q is constant. The sinking velocity ranged between 10 and 200 $m d^{-1}$. The steepest decrease in ΔC occurred at low sinking velocities, where the r_0 :DBL thickness ratio is low, and the relative decrease in DBL thickness becomes large at increasing flow velocity in the vicinity of the aggregate.

Discussion

The Sherwood number is often used in biological oceanography to estimate the potential increase in interface fluxes

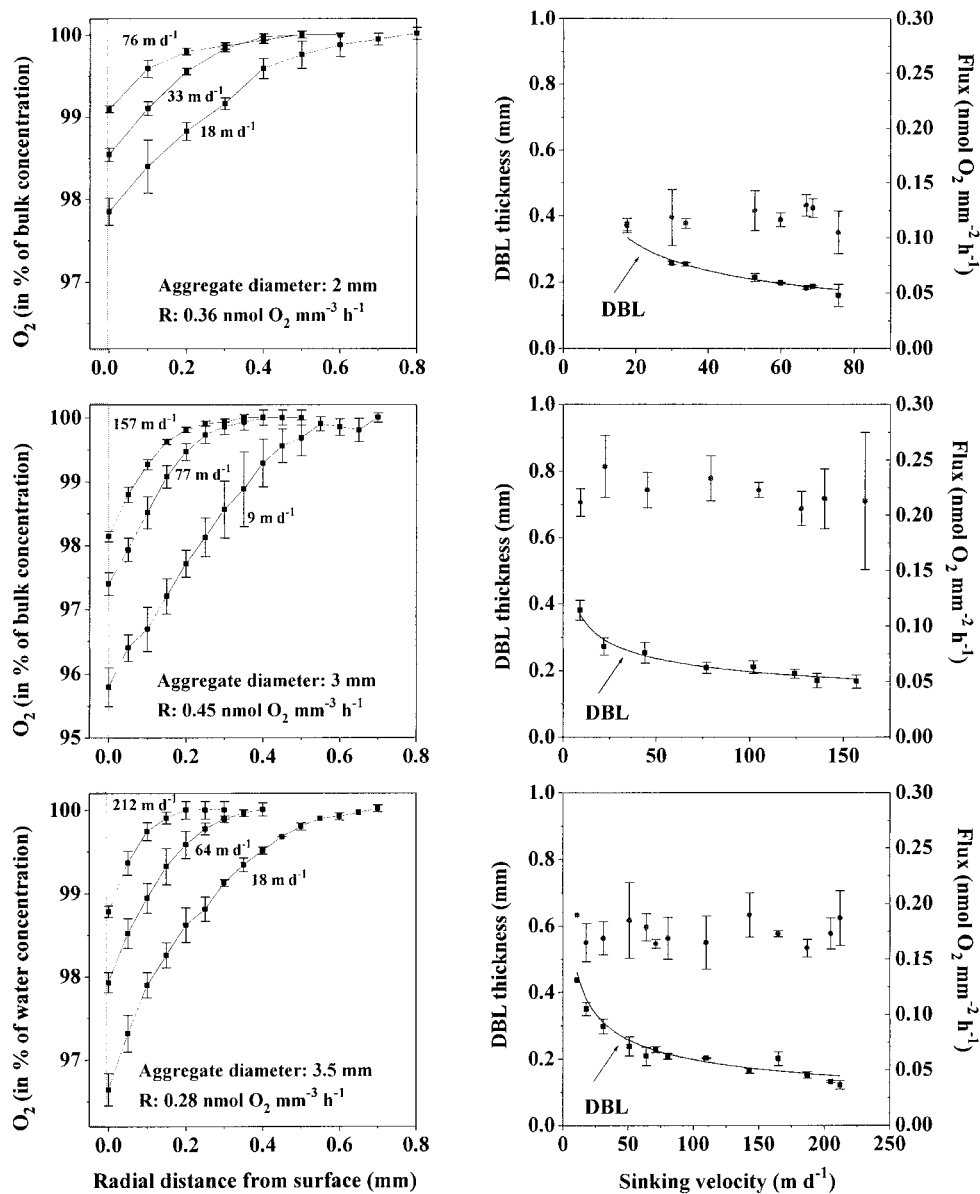


Fig. 5. Radial oxygen distributions along equator of three different aggregates at different flow velocities (left panel) and the DBL thickness and oxygen fluxes as a function of sinking velocity in the same aggregates (right panel). Each measuring point represents the mean value, with the SD of the mean value shown as bars ($n = 3$).

as particles sink through the water column. In such model calculations, however, it is assumed that the biological processes are transport limited rather than reaction limited (Csanady 1986; Karp-Boss et al. 1996; Brzezinski et al. 1997). The present study demonstrates that the diffusive boundary layer surrounding sinking aggregates decreases inversely proportional to the Sherwood number, whereby the exchange of solutes between aggregates and the surrounding water is facilitated during sedimentation. Flow and diffusion in the vicinity of sinking aggregates efficiently covered the oxygen demand of the attached biota, and the oxygen uptake was reaction limited in sinking aggregates of different sources and at different temperatures.

Oxygen transport limitation occurs where the oxygen demand exceeds the potential oxygen fluxes at the aggregate-water interface, and all oxygen is consumed at the aggregate surface. The half-saturation constant, K_m , for oxygen respiration is $\sim 0.1\text{--}3 \mu\text{M } O_2$ in heterotrophic bacteria, ciliates, and amoeba (Focht and Verstraete 1977; Fenchel and Finlay 1995). The transport-limited diffusive oxygen flux was calculated for different aggregate sizes (Eq. 4) from size-specific sinking velocities measured in situ (Alldredge and Gottschalk 1988), the bulk Sh (Eq. 2) and the oxygen solubility and diffusion coefficient at 4°C and 20°C. Transport-limited diffusive fluxes are relatively independent on temperature, because the temperature-dependent kinematic viscosity of

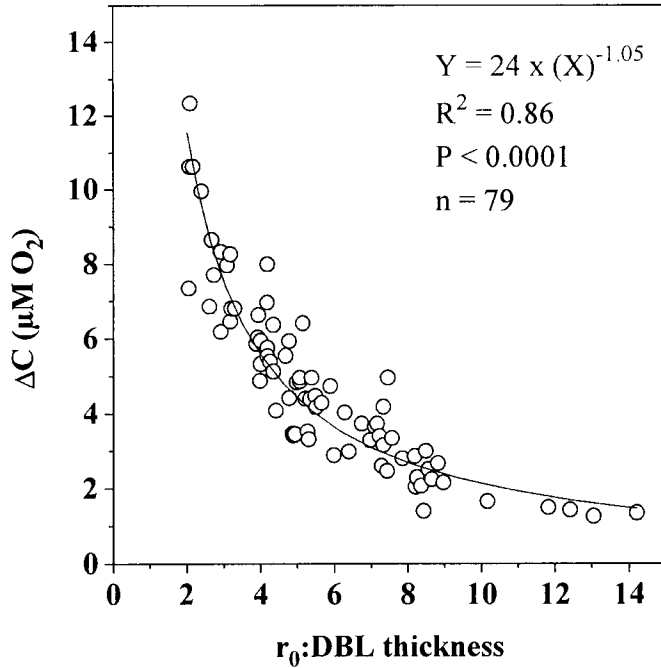


Fig. 6. The concentration difference across the aggregate-water interface, ΔC , as a function of the ratio between aggregate radius and DBL thickness.

sea water, the oxygen diffusion coefficient, and solubility balance in the combined temperature effect (Fig. 7). The viscosity effect on sinking velocity is not included in the calculations. To which extent the higher viscosity of sea water at low temperatures compared with that at high temperatures decreases sinking velocity is difficult to predict, because aggregates do not follow Stokes settling velocities (Allredge and Gotschalk 1988).

It has been argued that high concentrations of organic substrates in particles and aggregates make oxygen availability the most likely limiting factor in the remineralization process (Csanady 1986). I compiled size-specific respiration rates measured in field-sampled and lab-generated aggregates and compared those with the potential diffusive oxygen supply calculated for different concentrations of oxygen in the surrounding water, average size-specific sinking velocities, and the Sherwood number, as described above (Fig. 8). Aggregate sources, size, and sinking velocity are shown in Table 1. The transport-limited oxygen supply increases 26-fold because of diffusion and flow in the vicinity of aggregates when the diameter increases 10-fold, and the oxygen gradients are generally 10- to 100-fold lower than those determined by the transport-limited oxygen supply at 250 μM oxygen in the surrounding water. The transport-limited supply of oxygen is proportional to ambient oxygen concentrations. Anoxic aggregates in the 0.5–10 mm size range are, therefore, more likely to occur in the oxygen minimum zone of the ocean and in estuaries, as was previously suggested by other studies (Shanks and Reeder 1993; Ploug et al. 1997, 1999).

The DOC, particulate organic carbon (POC), and particulate organic nitrogen (PON) content of field-sampled ag-

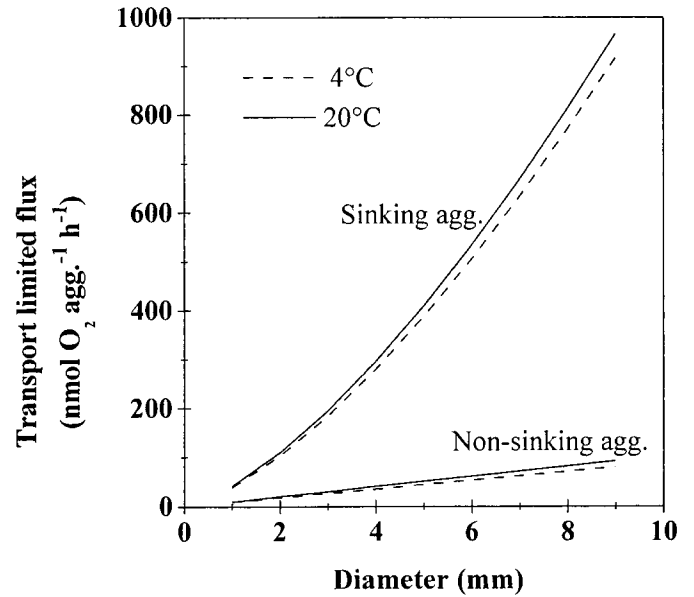


Fig. 7. Size-specific transport-limited flux at 4°C and 20°C.

gregates increased proportional to (aggregate diameter)^{-1.5}; i.e., the substrate content increases ~ 30 -fold when the diameter increases 10-fold (Allredge 1998, 2000). Hence, mass transfer scales approximately like substrate content with increasing aggregate size. Roller tank aggregates show higher respiration rates compared with field-sampled aggregates of similar sizes, and the respiration rates on roller-tank aggregates scale differently with aggregate size compared with those on field-sampled aggregates (Fig. 8). This may be explained by the fact that roller tank aggregates often are more compact than field-sampled aggregates, and roller tank aggregates have a higher size-specific carbon and nitrogen content compared with field-sampled aggregates. The car-

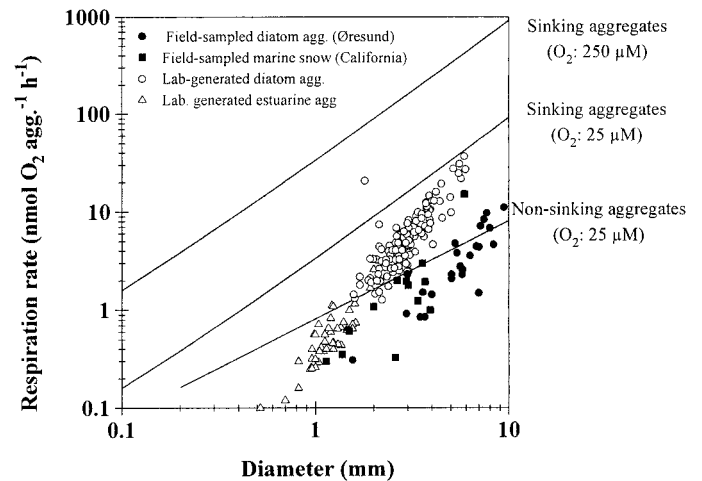


Fig. 8. Measured respiration rates in aggregates of different sources as a function of aggregate size (symbols). The solid lines represent the transport-limited oxygen supply as a function of ambient oxygen concentrations, aggregate size, and average size-specific sinking velocity (Allredge and Gotschalk 1988).

Table 1. Characteristics of source, size, and sinking velocity of field-sampled and lab-generated aggregates.

Aggregate source	Location	Diameter (mm)	U (m d ⁻¹)	No. of aggregates	Temperature (°C)	Reference
Diatoms (Field)	Øresund, Denmark	1.6–9.5	50–180	25	7	This study
Diatoms (Lab)	Cultures	2.6–5.9	45–170	150	15	This study; Ploug and Grossart (2000)
Marine snow (Field)						
with gelatinous mucus	Southern California Bight	1.2–5.9	10–65	13	16	Ploug et al. 1999
Marine snow (Field)						
Diatoms or detritus with gelatinous mucus	Santa Barbara Channel Southern California Bight	0.5–20	20–200	80	15–16	Allredge and Gotschalk 1988
Estuarine aggregate (Lab)	Weser, Germany	0.5–2.0	45–190	43	22	Grossart and Ploug 2000

bon-specific respiration rates, however, have been shown to be relatively similar in aggregates sampled in the field and produced in roller tanks, and community respiration increased proportional to POC and PON content in lab-generated diatom aggregates (Ploug and Grossart 2000). Oxygen concentrations within field-sampled marine snow were >90% of air-saturation although bacterial abundance were up to 2000-fold higher on aggregates compared to that in the surrounding water, and carbon-specific community respiration rates were 0.12 d⁻¹ (Ploug et al. 1999). Respiration within roller tank aggregates composed of freeze-thawed diatoms or fresh zooplankton detritus with high substrate content decreases exponentially during time proportional to POC and PON content, and respiration is, thus, likely substrate limited (Ploug et al. 1997; Ploug and Grossart 2000; Grossart and Ploug 2001).

Oxygen respiration rates were calculated assuming molecular diffusion to be the sole process of mass transfer within the aggregates, and the oxygen dynamics could be explained by mass transfer to spheres impermeable to flow. Theoretical studies have shown that interstitial fluid velocities within 7–20 mm large, fast-settling diatom aggregates may be in the order of 20–200 $\mu\text{m s}^{-1}$ (Logan and Hunt 1987; Logan and Alldredge 1989). An interstitial fluid flow would imply that the total oxygen uptake by aggregates is higher than the diffusive oxygen uptake measured from the oxygen gradients at the aggregate-water interface, and mass transfer to and from sinking aggregates would be even more efficient than that measured in this study. Previous studies of roller tank aggregates have shown that 80% of the time-dependent decrease in organic carbon content is explained by respiration, under the assumption that molecular diffusion of oxygen to be the sole process of mass transfer within aggregates (Ploug and Grossart 2000) and interstitial fluid flow within large, porous diatom aggregates cannot be excluded. However, interstitial fluid flow produces less steep oxygen gradients within aggregates compared with those that develop at pure diffusion, given similar respiration rates. The oxygen gradients and respiration rates measured by micro-sensors are, thus, conservative estimates.

Anoxia has been demonstrated in mm-large crustacean fecal pellets attached to large marine snow (Allredge and Cohen 1987), and it has been considered to be a common phenomenon in aggregates (Bianchi et al. 1992; Shanks and Reeder 1993; Karl and Tilbrook 1994). It has also been sug-

gested as an explanation of low production rates by aggregate-attached bacteria (Azam et al. 1993). However, later studies have shown that anoxic conditions may be an ephemeral phenomenon, only, in the bulk volume of sinking aggregates at high ambient oxygen concentrations (Ploug et al. 1997). Bacterial production measured in 1–4-mm large aggregates can be 5- to 10-fold higher during suspension/sinking compared with that measured in sedimented aggregates, partly because the diffusion distance for radio tracers into the aggregates is significantly reduced during suspension/sinking (Ploug and Grossart 1999, 2000). Respiration is tightly linked to bacterial production measured on the same aggregates, and the net growth efficiencies can be up to 0.50 \pm 0.10 (Grossart and Ploug 2000, 2001). The present study demonstrates that mass transfer and, hence, solute exchange at the aggregate-water interface is an efficient process during sedimentation. Remineralization of 0.5–10-mm large aggregates by attached biota is, therefore, determined by substrate quantity and quality rather than by oxygen transport limitation during sedimentation outside oxygen minimum zones in the ocean.

References

- ALLDREDGE, A. L. 1998. The carbon, nitrogen and mass content of marine snow as a function of aggregate size. *Deep-Sea Res. I* **45**: 529–541.
- . 2000. Interstitial dissolved organic carbon (DOC) concentrations within sinking marine aggregates and their potential contribution to carbon flux. *Limnol. Oceanogr.* **45**: 1245–1253.
- , AND Y. COHEN. 1987. Can microscale chemical patches persist the sea? Microelectrode study of marine snow and fecal pellets. *Science* **235**: 689–691.
- , AND C. C. GOTSCHALK. 1988. In situ settling behavior of marine snow. *Limnol. Oceanogr.* **33**: 339–351.
- , AND M. SILVER. 1988. Characteristics, dynamics and significance of marine snow. *Prog. Oceanogr.* **20**: 41–82.
- AZAM, F., D. C. SMITH, G. F. STEWARD, AND Å. HAGSTRÖM. 1993. Bacteria-organic matter coupling and its significance for oceanic carbon cycling. *Microb. Ecol.* **28**: 167–179.
- BIANCHI, M., D. MARTY, J.-L. TEYSSIÉ, AND S. W. FOWLER. 1992. Strictly aerobic and anaerobic bacteria associated with sinking particulate matter and zooplankton fecal pellets. *Mar. Ecol. Prog. Ser.* **88**: 55–60.
- BROECKER, W. S., AND T. H. PENG. 1974. Gas exchange rates between air and sea. *Tellus* **26**: 21–35.
- BRZEZINSKI, M. A., A. L. ALLDREDGE, AND L. M. O'BRYAN. 1997.

- Silica cycling within marine snow. *Limnol. Oceanogr.* **42**: 1706–1713.
- CARON, D. A., P. G. DAVIS, P. LAURENCE, L. P. MADIN, AND J. M. SIEBURTH. 1986. Enrichment of microbial populations in macroaggregates (marine snow) from surface waters of the North Atlantic. *J. Mar. Res.* **44**: 543–565.
- CSANADY, G. T. 1986. Mass transfer to and from small particles in the sea. *Limnol. Oceanogr.* **31**: 237–248.
- EISMA, D. 1993. Suspended matter in the aquatic environment. Springer.
- FENCHEL, T., AND B. J. FINLAY. 1995. Ecology and evolution in anoxic worlds. Oxford Univ. Press.
- FOTH, D. D., AND VERSTRAETE, W. 1977. Biochemical ecology of nitrification and denitrification. *Adv. Microbiol. Ecol.* **1**: 135–214.
- FOWLER, S. W., AND G. A. KNAUER. 1986. Role of large particles in the transport of elements and organic compounds through the oceanic water column. *Prog. Oceanogr.* **16**: 147–194.
- GROSSART, H.-P., AND H. PLOUG. (2000) Bacterial production and growth efficiencies: Direct measurements on riverine aggregate. *Limnol. Oceanogr.* **45**: 436–445.
- , AND ———. (2001) Microbial degradation of organic carbon and nitrogen on diatom aggregates. *Limnol. Oceanogr.* **46**: 267–277.
- , AND M. SIMON. 1993. Limnetic macroscopic organic aggregates (lake snow): Occurrence, characteristics, and microbial dynamics in Lake Constance. *Limnol. Oceanogr.* **38**: 532–546.
- HANSEN, P. J. 1989. The red tide dinoflagellate *Alexandrium tamarense*: Effects on behaviour and growth of a tintinnid ciliate. *Mar. Ecol. Prog. Ser.* **53**: 105–116.
- KARL, D. M., AND B. D. TILBROOK. 1994. Production and transport of methane in oceanic particulate organic matter. *Nature* **368**: 732–734.
- KARP-BOSS, L., E. BOSS, AND P. A. JUMARS. 1996. Nutrient fluxes to planktonic osmotrophs in the presence of fluid motion. *Oceanogr. Mar. Biol. Annu. Rev.* **34**: 71–107.
- KIØRBOE, T., H. PLOUG, AND U. H. THYGESEN. 2001. Fluid motion and solute distribution around sinking aggregates. I. Small-scale fluxes and heterogeneity of nutrients in the pelagic environment. *Mar. Ecol. Prog. Ser.* **211**: 1–13.
- LEE, C., AND S. T. WAKEHAM. 1988. Organic matter in sea water: Biogeochemical processes. *Chemical Oceanography*. Academic Press.
- LOGAN B. E., AND A. L. ALLDREDGE. 1989. Potential for increased nutrient uptake by flocculating diatoms. *Mar. Biol.* **101**: 443–450.
- , AND J. R. HUNT. 1987. Advantage to microbes of growth in permeable aggregates in marine systems. *Limnol. Oceanogr.* **32**: 1034–1048.
- PLOUG, H., AND H.-P. GROSSART. 1999. Bacterial production and respiration on suspended aggregates—a matter of the incubation method. *Aquat. Microb. Ecol.* **20**: 21–29.
- , AND ———. 2000. Bacterial growth and grazing on diatom aggregates: Respiratory carbon turnover as a function of aggregate size and sinking velocity. *Limnol. Oceanogr.* **45**: 1467–1475.
- , ———, F. AZAM, AND B. B. JØRGENSEN. 1999. Photosynthesis, respiration, and carbon turnover in sinking marine snow from surface waters of Southern California Bight: Implications for the carbon cycle in the ocean. *Mar. Ecol. Prog. Ser.* **179**: 1–11.
- , AND B. B. JØRGENSEN. 1999. A net-jet flow system for mass transfer and microelectrode studies in sinking aggregates. *Mar. Ecol. Prog. Ser.* **176**: 279–290.
- , M. KÜHL, B. BUCHOLZ, AND B. B. JØRGENSEN. 1997. Anoxic aggregates—an ephemeral phenomenon in the pelagic environment. *Aquat. Microb. Ecol.* **13**: 285–294.
- REVSBECH, N. P. 1989. An oxygen microelectrode with a guard cathode. *Limnol. Oceanogr.* **34**: 474–478.
- SHANKS, A. L., AND E. W. EDMONDSON. 1989. Laboratory-made artificial marine snow: A biological model of the real thing. *Mar. Biol.* **101**: 463–470.
- , AND M. L. REEDER. 1993. Reducing microzones and sulfide production in marine snow. *Mar. Ecol. Prog. Ser.* **96**: 43–47.
- , AND J. D. TRENT. 1980. Marine snow: Sinking rates and potential role in vertical flux. *Deep-Sea Res.* **27**: 137–144.
- SHERWOOD, T. K., R. L. PIGFORD, AND C. R. WILKE. 1975. Mass transfer. McGraw-Hill.
- SMITH, D. C., M. SIMON, A. L. ALLDREDGE, AND F. AZAM. 1992. Intense hydrolytic activity on marine aggregates and implications for rapid particle dissolution. *Nature* **359**: 139–141.

Received: 8 May 2001

Accepted: 19 June 2001

Amended: 20 July 2001